Published in final edited form as:
Biochim Biophys Acta. 2012 July ; 1822(7): . doi:10.1016/j.bbadis.2012.03.010.

Overexpression of VMAT-2 and DT-diaphorase protects substantia nigra-derived cells against aminochrome neurotoxicity

Patricia Muñoz[a], **Irmgard Paris**[a,b], **Laurie H. Sanders**[c], **J. Timothy Greenamyre**[c], and **Juan Segura-Aguilar**[a,*]

[a]Molecular and Clinical Pharmacology, Faculty of Medicine, University of Chile, Santiago 8380453, Chile

[b]Universidad Santo Tomás, Viña del Mar 2561780, Chile

[c]Department of Neurology and Pittsburgh Institute for Neurodegenerative Diseases, University of Pittsburgh, Pittsburgh, PA 15260, USA

Abstract

We tested the hypothesis that both VMAT-2 and DT-diaphorase are an important cellular defense against aminochrome-dependent neurotoxicity during dopamine oxidation. A cell line with VMAT-2 and DT-diaphorase over-expressed was created. The transfection of RCSN-3 cells with a bicistronic plasmid coding for VMAT-2 fused with GFP-IRES-DT-diaphorase cDNA induced a significant increase in protein expression of VMAT-2 (7-fold; $P<0.001$) and DT-diaphorase (9-fold; $P<0.001$), accompanied by a 4- and 5.5-fold significant increase in transport and enzyme activity, respectively. Studies with synaptic vesicles from rat substantia nigra revealed that VMAT-2 uptake of ^{3}H-aminochrome 6.3 ± 0.4nmol/min/mg was similar to dopamine uptake 6.2 ± 0.3 nmol/min/mg that which were dependent on ATP. Interestingly, aminochrome uptake was inhibited by 2 μM lobeline but not reserpine (1 and 10 μM). Incubation of cells overexpressing VMAT-2 and DT-diaphorase with 20 μM aminochrome resulted in (i) a significant decrease in cell death (6-fold, $P<0.001$); (ii) normal ultra structure determined by transmission electron microscopy contrasting with a significant increase of autophagosome and a dramatic remodeling of the mitochondrial inner membrane in wild type cells; (iii) normal level of ATP (256 ± 11 μM) contrasting with a significant decrease in wild type cells (121 ± 11 μM, $P<0.001$); and (iv) a significant decrease in DNA laddering (21 ± 8 pixels, $P<0.001$) cells in comparison with wild type cells treated with 20 μM aminochrome (269 ± 9). These results support our hypothesis that VMAT-2 and DT-diaphorase are an important defense system against aminochrome formed during dopamine oxidation.

Keywords

Dopamine; Neuromelanin; VMAT-2; DT-diaphorase; Aminochrome; Parkinson's disease

1. Introduction

Vesicular monoamine transporter-2 (VMAT-2) is able to take up dopamine into monoaminergic vesicles by using a vesicular proton pump associated to ATPase that under

*Corresponding author at: Molecular and Clinical Pharmacology, ICBM, Faculty of Medicine, Independencia1027, Santiago-7, Chile. Tel.: +56 2 978 6057; fax: +56 2 737 2783. jsegura@med.uchile.cl (J. Segura-Aguilar).

hydrolysis of ATP to ADP and Pi one proton (H^+) is translocated into the vesicle, generating an electrochemical gradient of protons. VMAT-2 uses this electrochemical gradient to take up one molecule of dopamine by releasing 2 protons [1,2]. This electrochemical gradient creates a low pH environment inside the monoaminergic vesicles estimated to be 2 to 2.4 pH units lower than in the cytosol [3], where the protons of dopamine hydroxyl groups are very hard bound to the oxygen, preventing dopamine oxidation. However, in the cytosol the protons of dopamine hydroxyl groups can dissociate and in the presence of oxygen dopamine oxidizes spontaneously without the necessity of metalion catalysis [4]. Dopamine oxidation to aminochrome catalyzed by oxygen is accompanied with the formation of superoxide radicals that can enzymatically or spontaneously generate hydrogen peroxide, the precursor of hydroxyl radicals. This oxidative mechanism of dopamine can be potentiated by drugs such as methamphetamine. VMAT-2 is able to take up methamphetamine into monoaminergic vesicles, inducing the release of dopamine to the cytosol that is an important event for methamphetamine neurotoxicity. The role of cytosolic dopamine in methamphetamine neurotoxicity has been supported by the fact that the inhibition of dopamine synthesis protects against methamphetamine neurotoxicity while the inhibition of VMAT-2 and monoamine oxidase exacerbate methamphetamine neurotoxicity [for review see 5].

Dopamine oxidation to aminochrome and its polymerization to neuromelanin seems to be a natural occurring process which accumulates with age [6,7]. Motor symptoms in Parkinson's disease are primarily the result from a selective loss of the neuromelanin-containing dopaminergic neurons of the substantia nigra while the unpigmented dopaminergic neurons are spared [8,9]. However, the question is why melanin containing dopaminergic neurons degenerate during Parkinson's disease when the neuromelanin formation itself is not neurotoxic. One possible explanation is that aminochrome is able to participate in neurotoxic reactions such as (i) the formation of adducts with alpha synuclein to produce and stabilize the formation of neurotoxic protofibers [10,11]; (ii) inducing mitochondrial dysfunction [12]; (iii) inactivation of proteosomal system [13,14]; (iv) disruption of cytoskeleton architecture [15]; and (v) formation of reactive oxygen species [16].

A complete knockout of VMAT2 (−/−) induces that mice move little, feed poorly, and die within a few days after birth while amphetamine increases movement, promotes feeding, and prolongs their survival [17]. VMAT2-deficient animals have decreased motor function, progressive deficits in olfactory discrimination, shorter latency to behavioral signs of sleep, delayed gastric emptying, anxiety-like behaviors at younger ages, and a progressive depressive-like phenotype [18]. Overexpression of VMAT-2 decreases cytosolic dopamine and inhibit neuromelanin synthesis, preventing dopamine oxidation to *o*-quinones [19]. Experiments done with human brain tissues support this idea since they found an inverse relationship between the level of expression of VMAT-2 and the amount of neuromelanin and the vulnerability to neurodegeneration in Parkinson's disease [20]. Therefore, VMAT-2 should play a protective role in dopaminergic neuron by preventing dopamine oxidation in the cytosol to aminochrome.

DT-Diaphorase (EC.1.6.99.2) is the unique flavoenzymes that catalyzes the two-electron reduction of aminochrome to leukoaminochrome and that can use both NADH and NADPH as electron donators [21]. This reaction is neuroprotective since it prevents one-electron reduction to leukoaminochrome *o*-semiquinone radical that it's extremely reactive with oxygen and neurotoxic [15,16,22–24]. DT-Diaphorase has been reported to prevent the cytoskeleton disruption [15], mitochondria damage [16,24], the formation of alpha synuclein protofibrils [25,26] and protects against aminochrome-induced proteasome inhibition [13]. Therefore, the aim of this work was to investigate the possible protective role of both of

VMAT-2 and DT-diaphorase against aminochrome neurotoxicity by creating a cell line with high expression of VMAT-2 and DT-diaphorase.

2. Materials and methods

2.1. Chemicals

Dopamine, reserpine, dicoumarol, DME/HAM-F12 nutrient mixture (1:1) and Dulbecco's phosphate buffered saline (PBS) were purchased from Sigma Chemical Co. (St Louis. MO. USA). Lobeline was obtained from Fluka. Calcein AM and ethidium homodimer-1 were obtained from Molecular Probe (Eugene. OR. USA). Thermoscript RT-PCR system and Taq DNA polymerase were obtained from Life Technologies (California. USA). Trizol reagent was obtained from Invitrogen (California. USA). The primers were obtained from T-A-G-Copenhagen A/S (Copenhagen. Denmark).

2.2. Preparation of synaptic vesicles and uptake

The purification of presynaptic vesicles was performed by using a Synaptic Vesicles Isolation KIT (Sigma-Aldrich Co., St. Louis. USA). After the gradient centrifugation, the protein concentration of the fraction containing synaptic vesicles was determined by Bradford method. Synaptic vesicles (2.5 μg protein) were incubated at 37 °C during 0, 60, 90 and 120 min in a buffer containing 25 mM HEPES, 100 mM potassium tartrate, 100 mM sodium tartrate, 1.7 mM ascorbic acid, 0.05 mM EGTA, 0.1 mM EDTA, and 2 mM ATP-Mg^{+2} at pH 7.5 in the presence of 50 nM ^{3}H-dopamine or ^{3}H-aminochrome. The samples were filtrated with a Sephadex G-25 to remove extracellular ^{3}H-dopamine or ^{3}H-aminochrome. The vesicles were disrupted by adding RIPA buffer and the isotopes were measured the counts per minute by using scintillate instrument.

2.3. Cell culture

The RCSN-3 cell line was derived from the substantia nigra of a 4-month-old normal Fisher 344 rat. The RCSN-3 cell line grows in monolayer with a doubling time of 52 h at a plating efficiency of 21% and a saturation density of 56,000 cells/cm^2 when kept in normal growth media composed of: DME/HAM-F12 (1:1), 10% bovine serum, 2.5% fetal bovine serum, and 40 mg/l gentamicine sulfate [27,28]. Cultures were kept in an incubator at 37 °C with 100% humidity and an atmosphere of 10% CO_2.

2.4. Cell transfection

The OmicsLink™ bicistronic plasmid pVMAT2GFPDTwith internal ribosome entry site (IRES) was used as expression vector systems of human synaptic vesicle monoamine transporter (accession no.: L09118), 1545 bp length fused in the C-terminal with GFP and *Homo sapiens* DT-diaphorase (NAD(P)H dehydrogenase quinone; accession no: NM_000903), and 825 bp length (GeneCopoeia). The transfection solutions was prepared by mixing 50 mM HEPES buffer, 30 mM NaCl, 1.5 mM Na_2HPO_4 pH 6.9, DNA plasmid and 2.5 M $CaCl_2$ and incubated at room temperature during 20 min. RCSN-3 cells in 60% confluence were transfected with this solution added slowly and mixing gently. The cells were incubated during 48 to 72 h at 37 °C.

2.5. Dot blot

Dot blots were performed by using a Bio-Rad Bio-Dot dot-blot apparatus assembled with a nitrocellulose membrane that previously was immersed in 20mM Tris pH 7.6 containing 136 mM NaCl was added to each well before the addition of 50–200 μl samples containing 50 μg protein. The vacuum connected to the dot blot equipment is allowed to continue until the membrane is dry. The nitrocellulose membrane was blocked by incubating the min

20mMTris pH 7.6 containing 136 mM NaCl, 0.1% Tween 20, low fat milk 5% during 3 h at room temperature with gently shaking. Wash the membrane 3 times during 5 min by using a solution of 20mM Tris pH 7.6 containing 136mM NaCl, 0.1% Tween 20. Incubate the membrane in a solution of 20mM Tris pH 7.6 containing 136 mM NaCl, 0.1% Tween 20, 5% BSA and polyclonal antibodies against DT-diaphorase diluted 1:1000 (SC-7012, Santa Cruz Biotechnology Inc). VMAT-2 diluted 1:1000 (AB1767, Millipore Chemicon) and actin diluted 1:1000 (SC-1615, Santa Cruz Biotechnology Inc). The membrane were washed 3 times 5 min and incubated in 20mM Tris pH 7.6 containing 136 mM NaCl, 0.1% Tween 20, 5% BSA and secondary antibody conjugated with HRP (horseradish peroxidase) diluted 1:10,000. The quantification of dot blot bands was performed by scanning the nitrocellulose membranes with scion image program (NIH) and they were expressed as pixels.

2.6. Determination of GFP fluorescence with confocal microscopy

Cover slips were mounted on to slides with fluorescent mounting medium (Dako, Carpinteria, CA. USA) and kept in the dark at 4 °C. Confocal microscopy (Zeiss, Göttingen. Germany; model LSM-410 Axiovert-100) was used to study the cells. Sample illumination was carried out via a He–Ne laser with 543-nm excitation filter and emission filter over 560 nm. The nuclei were marked with DAPI staining.

2.7. VMAT-2 activity determination

VMAT-2 activity was determined by measuring ^{3}H-dopamine transport in RCSN-3 and RCSN3VMATGFPDT cells with stable overexpression of VMAT2. The cells were harvested and collected by centrifugation (2000 rpm for 5 min) in PBS, resuspended at 1.25 × 10^{6} cells/ml in KT-HEPES buffer (25 mM HEPES; 100 mM potassium tartrate; 0.1 mM EDTA pH 7.5 at 25 °C) plus 10 μM digitonin and incubated at room temperature for 10 min. Cells were then collected by centrifugation (3000 rpm for 5 min) and resuspended at 1.25 × 10^{6} cells/ml in KT-HEPES buffer. For [^{3}H]dopamine uptake, the cell suspension (200 μl) was incubated with KT-HEPES buffer containing 5 mM ATP-Mg^{2+} and 50 nM [^{3}H]dopamine at temperature 37 °C for 45min and the reaction terminated at 12,500 rpm for 15 min at 0 °C followed by addition of 0.1% SDS to each cell pellet. Non-specific uptake was determined with RCSN-3 cells wild type in the presence of 10 μM tetrabenazine (American Radiolabeled Chemicals. Inc., St. Louis. MO). Radioactivity was quantified with a scintillation spectrometer. The data was normalized by measuring protein concentration with Biuret method.

2.8. DT-Diaphorase activity determination

DT-Diaphorase activity in RCSN-3 and RCSN3VMAT2GFPDT was determined in Tris/HCl buffer at pH 7.5 containing 0.08% Triton X-100 by using 500 μM NADH or 500 μM NADPH as electron donor, 77 μM cytochrome C and 10 μM menadione as electron acceptor. The reaction was measured spectrophotometrically by following the reduction of cytochrome C, which continuously reoxidize the reduced menadione at 550 nm and employing an extinction coefficient of 18.5 mM^{-1} cm^{-1}. DT-Diaphorase activity was calculated by inhibiting the quinone reductase activity with dicoumarol [29].

2.9. Cell death determination

The cells were incubated with cell culture medium but in the absence of bovine serum and phenol red for 24 h. The concentration used for toxicity experiments was 20 μM aminochrome in the presence or absence of 100 μM dicoumarol or 2 μM lobeline. For control conditions, we used 20 μM aminochrome, 2 μM lobeline or 100 μM dicoumarol incubated alone. The cells were visualized at 100 × magnification in a Nikon Diaphot inverted microscope equipped with phase contrast and fluorescence optics. The toxicity was

measured by counting live and dead cells after staining with 0.5 μM Calcein AM and 5 μM ethidium homodimer-1 for 45 min at 37 °C in the darkness. Calcein AM is a marker for live cells and ethidium homodimer-1 that intercalates in the DNA of dead cells is a marker for cell death. The cells were counted in a phase contrast microscope equipped with fluorescence, using the following filters: Ethidium homodimer-1 510–560 nm (excitation) and LP-590 nm (emission); Calcein AM 450–490 nm (excitation) and 515–565 nm (emission). For experiments to study autophagy effect on cell death the cells were incubated with 10 μM vinblastine or 10 μM rapamycin.

2.10. Transmission electron microscopy

After the treatments, RCSN-3 and RCSN3VMAT2GFPDT cells were washed three times with PBS pH 7.4 and fixed in 3% glutaraldehyde for 240 min, washed 3 times and post-fixed in osmium tetra oxide 2% for 60 min at room temperature. The cells were dehydrated in an ascending ethanol battery ranging from 20 to 100% and were later placed in 100% ethanol for 10 min and finally embedding in epon-812 resin. Ultrathin sections were made and impregnated with 4% uranyl acetate and Reynold's lead citrate. The sections were visualized in a Zeiss EM-900 transmission electron microscope at 50 kV photographed, the negatives were scanned at 600 × 600 ppi resolution and the images obtained were analyzed later in a PC compatible computer using customized software.

2.11. GFP-LC3 plasmid transfection

Cells were grown in culture medium in 24-well plates for 48 h after being transfected with green fluorescent-protein light chain 3 (GFP-LC3) plasmid (gift from Zsolt Tallocky PhD, Columbia University Medical Center). To form the transfection complex, we used 2 μl Fugene HD transfection reagent (Roche Diagnostics) and 0.5 μg GFP-LC3 plasmid DNA in 25 μl total volume of medium for each plate, kept in the dark for 15 min. Thereafter, the transfection complex in 150 μl culture medium was added to each plate and incubated for 1 h. Then, 350 μl culture medium was added to each plate and cultured for two days. The cells were analyzed by using a confocal microscopy.

2.12. DNA isolation and quantitative polymerase chain reaction (QPCR) of nuclear DNA (nDNA) fragment

Cells were isolated as previously described [23]. QPCR method to detect nuclear DNA damage was performed as previously described [30,31,23]

2.13. DNA fragmentation

RCSN-3 and RCSN3VMAT2GFPDT cells were incubated with 20 μM aminochrome; 20 μM aminochrome and 100 μM dicoumarol; 20 μM aminochrome and 2 μM lobeline. As control the cells were treated with 2 μM lobeline or 100 μM dicoumarol for 48 h. The medium was removed and the cells were incubated in 90 μl 10% SDS and 810 μl buffer TE (10 mM Tris HCl, 1 mM EDTA, pH 8) for 2–5 min at room temperature. The extracted cells were placed in a tube containing 900 μl saturated phenol and centrifuged at 14,000 rpm for 10 min at 4 °C. The aqueous phase was extracted by addition of 900 μl of saturated phenol and centrifuged at 14,000 rpm for 10 min at 4 °C. This procedure was performed twice. The aqueous phase was mixed with 900 μl 24:1 chloroform: isoamilic ethanol and centrifuged at 14,000 rpm for 10 min 4 °C. The aqueous phase was removed and resuspended in 90 μl 3 M sodium acetate pH 5.2 and isopropanol to fill the tube, incubated at −20 °C for 24 h and centrifuged at 14,000 rpm for 15 min at 4 °C. The pellet was resuspended in 70% ethanol and centrifuged at 14,000 rpm for 10 min at 4 °C. The precipitate was dried at room temperature and resuspended in TE. The amount of DNA was measured spectrophotometrically, and 4 μg was run on an agarose gel. Electrophoresis was carried out

in 2.5% agarose gels in buffer TBE (45 mM Tris-base, 45 mM boric acid and 1.6 mM EDTA). Quantification was performed by scanning the area of separation of DNA under 10,000 bp by using ScionImage software (NIH) and the pixels were plotted.

2.14. Data analysis

All data were expressed as mean ± SD values. The statistical significance was assessed using analysis of variance (ANOVA) for multiple comparisons and Student's *t*-test.

3. Results

3.1. Aminochrome uptake

We have isolated synaptic vesicles from rat brain to study the ability of VMAT-2 to take up ^{3}H-aminochrome. Synaptic vesicles are able to take up ^{3}H-aminochrome that increase with time at similar rate to ^{3}H-dopamine (Fig. 1A). No significant differences between ^{3}H-dopamine (6.12 ± 0.1 nmol/min/mg) and ^{3}H-aminochrome (6.15 ± 0.05 nmol/min/mg) was observed when synaptic vesicles were incubated during 120 min. ^{3}H-Dopamine (30 nM) uptake into substantia nigra synaptic vesicles was inhibited by 10, 50, and 100 μM aminochrome (37, 45 and 67% inhibition; $P<0.05$, 0.05 and 0.01, respectively). As a positive control 10 μM dihydrotetrabenazine was used resulting in 81% inhibition of ^{3}H-dopamine uptake (Fig. 1B). The cells incubated with 1 μM reserpine induced a strong inhibition of ^{3}H-dopamine uptake (82%; $P<0.001$) while the inhibition of ^{3}H-aminochrome uptake was lower (23%; $P<0.01$). The incubation of 1 μM reserpine at 4 °C did not increase the uptake inhibition of ^{3}H-dopamine (88%; $P<0.001$ compared to the control) while under these conditions ^{3}H-aminochrome uptake was strong inhibited (74%; $P<0.001$ compared to the control). Both ^{3}H-dopamine and ^{3}H-aminochrome uptake was near complete inhibition when 1 μM reserpine was incubated in the absence of ATP (98%, $P<0.001$ and 97%, $P<0.001$, respectively) (Fig. 1C). We isolated synaptic vesicles from rat substantia nigra in order to increase the number of monoaminergic vesicles and we tested lobeline as inhibitor of VMAT-2. The incubation of monoaminergic vesicles with 2 μM lobeline inhibited both ^{3}H-dopamine (56%; $P<0.01$) and ^{3}H-aminochrome (61%; $P<0.01$) uptake. Incubation of monoaminergic vesicles with 2 μM lobeline at 4 °C resulted in inhibition of both ^{3}H-dopamine (91%; $P<0.001$) and ^{3}H-aminochrome (83%; $P<0.001$) uptake (Fig. 1D).

3.2. VMAT-2 and DT-diaphorase overexpression

The possible protective role of VMAT-2 and DT-diaphorase against aminochrome neurotoxicity was studied by increasing the expression of VMAT-2 and DT-diaphorase in RCSN-3 cells by transfecting the plasmid pVMAT2GFPDT coding for the cDNA of VMAT-2 fused to the C-terminal with the green fluorescence protein (GFP) and DT-diaphorase. Transfection of RCSN-3 cells with the plasmid pVMAT2GFPDT induced a significant increase in the expression of VMAT-2 (7-fold; $P<0.001$; Fig. 2B and C) and DT-diaphorase (9- fold; $P<0.001$; Fig. 2A and C) determined by using dot-blot technique. The transfected cells with pVMAT2GFPDT were selected by growing the cells in the presence of 250 μg/ml geniticine obtaining a cell line with green fluorescence as it can be observed in Fig. 2D (right). The enzymatic activity of DT-diaphorase in RCSN3VMAT2GFPDT-cells increased in 5.5-fold (6.6 ± 1 μmol/min/mg protein) in comparison with wild type RCSN-3 cells (1.2 ± 0.2 μmol/min/mg protein; $P<0.001$) and RCSN3GFP cells transfected with plasmid coding for GFP alone (1.2 ± 2 μmol/min/mg protein; Fig. 2E). RCSN3VMAT2GFPDTcells also exhibited a 4-fold increase in VMAT-2 activity ($P<0.001$; Fig. 2F).

3.3. Aminochrome-induced cell death

A significant decrease in cell death was observed in RCSN3VMAT2-GFPDT cells (5.5 ± 0.4%) incubated with 20 μM aminochrome during 24 h in comparison with RCSN-3 cells (34 ± 0.3%; P<0.001) and RCSN-3-GFP cells (29 ± 1%; P<0.01) incubated under the same conditions. The inhibition of DT-diaphorase by 100 μM dicoumarol in RCSN3VMAT2GFPDT incubated with 20 μM aminochrome increased the cell death (24 ± 1; P<0.001) in comparison with RCSN3VMAT2GFPDT incubated alone with 20 μM aminochrome, but when we compare the cell death between RCSN-3 cells incubated with 20 μM aminochrome and 100 μM dicoumarol (42 ± 1) with RCSN3VMAT2GFPDT incubated under the same conditions we can observe a significant decrease in cell death (P<0.001). A significant decrease in cell death in RCSN3VMAT2GFPDT (18 ± 1%; P<0.001) incubated with 2 μM lobeline and 20 μM aminochrome was observed in comparison with RCSN-3 cells (45 ± 0.2%) treated under the same conditions (Fig. 3). No significant cell death was observed in RCSN-3, RCSN-3-GFP and RCSN3VMAT2GFPDT cells treated with 100 μM dicoumarol (2.9 ± 0.1; 3.0 ± 0.2; 6.6 ± 1, respectively) or 2 μM lobeline (5 ± 0.1; 2.9 ± 1.4; 4.3 ± 1, respectively) (data not shown).

3.4. Aminochrome effect on autophagy

Transmission electron microscopy was performed to examine cellular changes at the ultrastructure level in order to obtain more information about the mechanism of cell death induced by aminochrome in the presence of dicoumarol or lobeline. The ultrastructure of RCSN-3 cells incubated with 20 μM aminochrome showed autophagy vacuoles with double membrane containing a dark pigment (Fig. 4D). RCSN-3 cells incubated with 20 μM aminochrome and 100 μM dicoumarol show autophagy vacuoles containing remainder of organelles such as mitochondria (Fig. 4F) or incubated with 20 μM aminochrome, 100 μM dicoumarol and 2 μM lobeline also show autophagy vacuoles (Fig. 4H). However, RCSN3VMAT2GFPDT cells treated with 20 μM aminochrome (Fig. 4E); 20 μM aminochrome and 100 μM dicoumarol (Fig. 4G); and 20 μM aminochrome and 2 μg lobeline (Fig. 4I) showed a normal ultrastructure without the presence of autophagy vacuoles (Fig. 4E, G and I). We analyzed the formation autophagosome vacuoles by transfecting RCSN-3 and RCSN3VMAT2GFPDT cells with a plasmid coding for LC3-GFP that produce green fluorescence. The treatment of RCSN-3 cells with 20 μM aminochrome; 20 μM aminochrome and 100 μM dicoumarol; or 20 μM aminochrome and 2 μM lobeline induces a significant increase in the number LC3 positive cells in comparison with untreated cells (25 ± 1, P<0.05; 37 ± 3, P<0.001; 39 ± 3, P<0.001 LC3 positive cells, respectively). The treatment with 20 μM aminochrome or 20 μM aminochrome and 100 μM dicoumarol in RCSN3VMAT2GFPDT did not induce a significant increase in LC3 positive cells (6 ± 2 and 7 ± 2), in comparison with control cells (6 ± 2 LC3 positive cells, respectively). No significant increase in LC3 positive cells was observed in RCSN3VMAT2GFPDT cells treated with 20 μM aminochrome and 2 μM lobeline; or 20 μM aminochrome, 100 μM dicoumarol and 2 μM lobeline (13 ± 2 and 14 ± 2 LC3 positive cells) in comparison with RCSN-3 control cells (Fig. 5A). To study the role of autophagy vacuoles on aminochrome induced cell death we used vinblastine that is an inhibitor of autophagosome fusion with lysosomes. The incubation of RCSN-3 cells with 20 μM aminochrome in the presence of 10 μM vinblastine induced a significant increase in cell death from 38 ± 2% to 48 ± 5% (P<0.05). Incubation of RCSN-3 cells with 20 μM aminochrome together with 100 μM dicoumarol in the presence of 10μM vinblastine also induced a significant increase in cell death (45 ± 1% and 51 ± 4% P<0.05, respectively). Incubation of RCSN-3 cells with 20 μM aminochrome together with 2 μM lobeline also induced a significant increase cell death in the presence of 10 μM vinblastine (61 ± 4%; P<0.001). However, in RCSN3VMAT2GFPDT cells the presence of 10 μM vinblastine induced a significant increase only in cells treated with 20 μM aminochrome alone (7.8 ± 0.2% to 36 ± 4%;

P<0.001) while no statistically significant differences were observed when the cells were treated with 20 μM aminochrome together with 100 μM dicoumarol or 20 μM aminochrome together with 2 μM lobeline (Fig. 5B). We used also rapamycin, an inducer of autophagy, to study the role of autophagy in RCSN3VMAT2GFPDT cells (Fig. 5C). A significant decrease in cell death was observed in RCSN-3 cells pre-treated with 10 μM rapamycin during 2 h prior addition of 20 μM aminochrome; 20 μM aminochrome and 2 μM lobeline; or 20 μM aminochrome and 100 μM dicoumarol (22 ± 2%, P<0.001; 32 ± 3%, P<0.0.01; 28 ± 3% cell death P<0.01, respectively) in comparison with cells without rapamycin pre-treatment. A significant decrease in cell death was also observed in RCSN3VMAT2GFPDT cells pre-treated with 10 μM rapamycin incubated with 20 μM aminochrome and 2 μM lobeline or 20 μM aminochrome and 100 μM dicoumarol compared with cell without pre-treatment. However, no significant differences were observed in RCSN3VMAT2GFPDT cells pre-treated with rapamycin and incubated with aminochrome alone in comparison with cells without pre-incubation with rapamycin.

3.5. Aminochrome effect on mitochondria

Dramatic changes in mitochondrial ultrastructure were observed in RCSN-3 cells treatedwith 20 μM aminochrome and 100 μM dicoumarol that included remodeling of the inner membrane conformation to a form abnormal vesicular mitochondria structure (see Fig. 6F, white arrow) contrasting with normal mitochondria ultra structure in RCSN3VAMT2GFPDT cells treated under the same conditions (Fig. 6G). RCSN-3 cells treated with 20 μM aminochrome and 2 μM lobeline also showed a dramatic remodeling of inner mitochondrial membrane (Fig. 6H, white head of arrows) contrasting with normal inner membrane of mitochondria in RCSN3VAMT2GFPDT cells treated under the same conditions (Fig. 6I). Normal mitochondria are observed in RCSN-3 cells incubated with cell culture medium (Fig. 6A); 100 μM dicoumarol (Fig. 6B); 2 μM lobeline and 20 μM aminochrome (Fig. 6H); and in RCSN3VAMT2GFPDT cells incubated with 20 μM aminochrome (Fig. 6E); 20 μM aminochrome and 100 μM dicoumarol (Fig. 6G); and 20 μM aminochrome and 2 μM lobeline (Fig. 6I). We measured ATP level in RCSN-3 cells and we found a significant decrease in cells treated with 20 μM aminochrome (121 ± 11 μM ATP; P<0.001); 20 μM aminochrome together with 100 μM dicoumarol (172 ± 6 μM ATP; P<0.001); or 20 μM aminochrome together with 2 μM lobeline (156 ± 7 μM ATP; P<0.001) in comparison with untreated RCSN-3 cells (278 ± 9 μM ATP). This result contrasts with lack of significant differences in RCSN3VAMT2GFPDT cells treated with 20 μM aminochrome (256 ± 11 μM ATP) compared to control cells. A significant decrease in ATP level was also observed in RCSN-3 and RCSN3VAMT2GFPDT cells treated with 20 μM aminochrome together with 100 μM dicoumarol (198 ± 15; P<0.001) or 20 μM aminochrome together with 2 μM lobeline (195 ± 25; P<0.01). The levels of ATP in RCSN-3 and RCSN3VAMT2GFPDT cells treated with 2 μM lobeline or 100 μM dicoumarol were 229 ± 20, 244 ± 8, 246 ± 6 and 245 ± 4 μM ATP (Fig. 7).

3.6. Aminochrome effect on DNA

We determined whether VMAT-2 and DT-diaphorase was protective against nuclear DNA damage in response to aminochrome treatment. In RCSN3VMAT2GFPDT cells treated with cell culture medium, nuclear DNA damage decreased relative to control RCSN-3 cells (−0.14 ± 0.01 lesions/10 kb; Fig. 8A). RCSN3VMAT2GFPDT cells treated with 100 μM aminochrome also showed decreased levels of nuclear DNA damage (0.34 ± 0.09 lesions/10 kb) relative to RCSN-3 cells treated under the same conditions (1.2 ± 0.01 lesions/10 kb; Fig. 8A). We determined DNA fragmentation in cells treated with 20 μM aminochrome in the presence of 2 μM lobeline and 100 μM dicoumarol by using DNA laddering technique. A significant decrease in DNA fragmentation was observed in RCSN3VMAT2GFPDT cells in comparison with RCSSN-3 cells treated with 20 μM aminochrome (8.2% of control;

P<0.05); 20 μM aminochrome and 100 μM dicoumarol (15% of control; P<0.05); 20 μM aminochrome and 2 μM lobeline (57% of control; P<0.05) and 20 μM aminochrome, 100 μM dicoumarol and 2 μM lobeline (30% of control; P<0.05; Fig. 8B).

4. Discussion

The molecular mechanism involved in the degeneration of the nigro-striatal system in Parkinson's disease is still unclear. However, it is generally accepted that mitochondrial dysfunction, aggregation of proteins such as alpha synuclein, dysfunction of protein degradation systems, oxidative stress and neuroinflammation are involved in the loss of dopaminergic neurons containing neuromelanin in Parkinson's disease. Aging is also an important risk factor for neuro-degenerative disorders including Parkinson's disease. Aging process can negatively influence these molecular mechanisms that underlie neurodegeneration in Parkinson's disease. The question is the identity of the neurotoxin that induces the neurodegeneration of nigrostriatal system; one may speculate that it is of endogenous origin due to the fact that neurodegeneration and disease progression is very slow and can take many years. The main reason why the neurotoxin should be of endogenous origin is that MPTP induces severe Parkinsonism symptoms in humans only 3 days after injection [32]. Therefore, it seems plausible that an endogenous neurotoxin generated inside of dopaminergic neurons containing neuromelanin is responsible for this slow degenerative process that take years, since an exogenous neurotoxin with high affinity for dopamine transport will affect extensive number of dopaminergic neurons inducing a rapid appearance of motor symptoms. One possible candidate for endogenous neurotoxin is aminochrome that is the product of dopamine oxidation and the precursor of neuromelanin. Dopamine oxidizes to dopamine *o*-quinone that is the precursor of aminochrome, which is a transient compound at physiological pH levels, since its amino chain spontaneously at physiological undergoes cyclization to form aminochrome [21]. Aminochrome is able to polymerize to form the neuromelanin pigment that is present in dopaminergic neurons. Neuromelanin accumulates with age [6,7] and it seems to be a normal event since dopaminergic neurons contain neuromelanin are present in individuals without the disease. Neuromelanin accumulates in double membrane vesicles where it plays a clear neuroprotective role while free neuromelanin has been found to induce neuroinflammation and neurodegeneration [33,34]. However, aminochrome is able to induce neurotoxicity by the following reactions: (i) the formation of adducts with proteins such as alpha synuclein [10,11], with the complexes I and III of the electron transport chain in mitochondria [12], with actin and α- and β-tubulin [15]. In addition, aminochrome inactivates parkin, that is a ubiquitin ligase 3 [35], tyrosine hydroxylase and human dopamine transporter [36,37]; and (ii) its one-electron reduction leukoaminochrome *o*-semiquinone radical with concomitant formation of superoxide, hydrogen peroxide and hydroxyl radical [16,23], inducing a redox cycling depleting NADH and oxygen required for ATP production. Aminochrome has been proposed to be the endogenous neurotoxin responsible of the slow and progressive neurodegeneration of dopaminergic neurons containing neuromelanin [23,38]. VMAT-2 mediated dopamine uptake into monoaminergic vesicles and therefore, will prevent dopamine oxidation and aminochrome neurotoxicity and DT-diaphorase prevents aminochrome one-electron reduction and the formation of adducts with proteins. Therefore, to study the protective role of VMAT-2 and DT-diaphorase against aminochrome neurotoxicity, we designed a plasmid containing an internal ribosome entry site (IRES) for coexpression of VMAT-2 fused to eGFP and DT-diaphorase. The expression of VMAT-2 and DT-diaphorase in RCSN3VMAT2GFPDT cells increased 7- and 9-fold and their activity increased in near 4- and 6-fold in comparison to RCSN-3 cells, respectively. This cell line seemed to be a good model cell line to study VMAT-2 and DT-diaphorase protective role in dopaminergic neurons (Fig. 9).

There are three ways to prevent aminochrome neurotoxicity: (i) preventing dopamine oxidation to aminochrome. In dopaminergic neurons, the intracellular dopamine is efficiently incorporated into monoaminergic vesicles by VMAT-2 for neuronal transmission or storage. Therefore, VMAT-2 mediated dopamine uptake into monoaminergic vesicles should be considered as a very important neuroprotective mechanism in dopaminergic neurons since the low pH inside the monoaminergic vesicles prevent dopamine oxidation to aminochrome. Dopamine synthesis occurs at the synaptic terminal catalyzed first by tyrosine hydroxylase that converts tyrosine to L-dopa and secondly aromatic amino acid decarboxylase that converts L-dopa to dopamine. There is evidence that VMAT-2 physically and functionally interacts with the enzymes responsible for DA synthesis [39], preventing the existence of free dopamine in the cytosol. However, the uptake of dopamine released during neurotransmission mediated by dopamine transporter will provide free intracellular dopamine but VMAT-2 will transport this dopamine into monoaminergic vesicles. Another mechanism to prevent free cytosolic dopamine is mediated by monoamino oxidase that is able to degrade free cytosolic dopamine by catalyzing the oxidative deamination of dopamine with concomitant formation of hydrogen peroxide. Inhibition of monoamine oxidase has been used in Parkinson's disease treatment in order to inhibit dopamine degradation [40]. Another mechanism to prevent accumulation of free cytosolic dopamine is the formation of neuromelanin [9]; (ii) preventing aminochrome participation in neurotoxic reactions such as adducts formation with proteins and one-electron reduction. Our results revealed that VMAT-2 is able to take up aminochrome at a similar rate as dopamine suggesting that VMAT-2 plays a double protective role against aminochrome neurotoxicity by preventing dopamine oxidation to aminochrome in the cytosol and by transporting cytosolic aminochrome into monoaminergic vesicles where aminochrome cannot form adducts with proteins or be one-electron reduced; and (iii) preventing one-electron reduction to leukoaminochrome *o*-semiquinone radical which is extremely reactive with oxygen by two-electron reduction of aminochrome catalyzed by DT-diaphorase [16,24,23]. DT-Diaphorase prevents aminochrome one-electron reduction and subsequent redox cycle between aminochrome and the leukoaminochrome *o*-semiquinone radical [41,42]. This redox cycle depletes NADH when flavoenzymes use NADH as electron donor during one-electron reduction of aminochrome inducing an energy collapse since NADH is required for ATP synthesis in the mitochondria. Our results support this idea since RCSN-3 cells incubated with aminochrome induced a significant decrease in ATP level (50%). DT-Diaphorase also prevents the formation of neurotoxic protofibrils during the formation of aminochrome adducts with alpha-synuclein [25,26]. DT-Diaphorase prevents the cytoskeleton disruption by preventing actin, α-tubulin and β-tubulin aggregation [10]. DT-Diaphorase also prevents mitochondrial damage [16,24] and aminochrome-induced proteasome inhibition [13].

Overexpression of VMAT-2 and DT-diaphorase in RCSN3VMAT2-GFPDT cells prevents ultrastructure damage in the presence of aminochrome since (i) ultrastructure of mitochondria was preserved in contrast to RCSN-3 cells showing remodeling of the inner membrane conformation. The lack of damage of mitochondria was also supported by the lack of effect of aminochrome on ATP level in RCSN3VMAT2GFPDTcells contrasting with a significant decrease of ATP level in RCSN-3 cells; (ii) the autophagy level in RCSN3VMAT2GFPDT cells treated with aminochrome was similar as the constitutive level of cells treated with cell culture medium determined by transmission electron microscopy and LC3-GFP positive autophagosome, suggesting that the incubation of cells with overexpression of both VMAT-2 and DT-diaphorase with aminochrome do not require an increase in autophagy. Autophagy is an intracellular degradation mechanism whereby organelles and proteins are transported by autophagy vacuoles into lysosomes for degradation and recycling [43–45]. Autophagy plays an important role in the elimination of damaged organelles such as mitochondria. It has been reported that aminochrome induces

autophagy [23]. An interesting finding from analysis of ultrastructure with transmission electron microscopy is the formation of a dark pigment inside of double membrane autophagy vacuoles in RCSN-3 cells treated both with aminochrome and an inhibitor of DT-diaphorase, contrasting with the lack of pigment in RCSN-3 cells incubated without DT-diaphorase inhibitor. These results suggest that DT-diaphorase inhibition preventing two-electron reduction of aminochrome is important for formation of neuromelanin.

To determine the role of autophagy on aminochrome-induced cell death in RCSN-3 and RCSN3VMAT2GFPDT cells we used vinblastine, an inducer of autophagosome accumulation by blocking the fusion of autophagy vacuoles and lysosomes [46] and rapamycin, an inducer of macroautophagy by inactivating mTor pathway [47]. In RCSN-3 cells aminochrome induces an increase in cell death in the presence of vinblastine and a decrease in cell death in the presence of rapamycin as it was expected [23]. However, in RCSN3VMAT2GFPDT cells aminochrome induces an increase in cell death in the presence of vinblastine but no significant differences were observed when the cells were incubated with rapamycin. A possible explanation for the lack of effect of rapamycin on cell death can be explained by low level of cell death induced by aminochrome (7 ± 1%) as a consequence of the protective effect of VMAT-2 and DT-diaphorase overexpression. Vinblastine induces an increase in aminochrome-dependent cell death both in RCSN-3 or RCSN3VMAT2GFPDT cells when DT-diaphorase was inhibited by dicoumarol and a decrease in cell death in the presence of rapamycin supporting the protective role of autophagy in aminochrome neurotoxicity [23]. However, vinblastine did not increase the cell death in RCSN3VMAT2GFPDT cells treated with aminochrome and lobeline, a result that we still have no explanation. Rapamycin induces a decrease in cell death both in RCSN-3 or RCSN3VMAT2GFPDT cells whenVMAT-2 was inhibited by lobeline suggesting that autophagy protect against aminochrome neurotoxicity.

Our results may explain why VMAT2-deficient in mice induces a progressive neurodegeneration in the substantia nigra coupled with α-synuclein accumulation [48,18] since a deficiency or knockdown of VMAT-2 will result in accumulation of free cytosolic dopamine [49] that autoxidizes to aminochrome inducing neurodegeneration accompanied with accumulation of α-synuclein aggregation. The increase in aminochrome concentration plays an important role in α-synuclein aggregation since aminochrome induces and stabilizes the formation of α-synuclein protofibers [10,11]. Exposure of mice with low expression of VMAT-2 (5–10%) to methamphetamine exacerbates the loss of dopamine transporter and tyrosine hydroxylase, accompanied with an increase in astrogliosis and protein carbonyl formation [50], probably as a consequence of dopamine release induced by methamphetamine [51]. VMAT2+/− mice were more sensitive to the neurotoxic effects of MPTP, since the VMAT2-mediated uptake of the neurotoxin into vesicles may play an important role in attenuating MPTP toxicity in vivo [52]. On the other side high-level expression of rat VMAT-2 induced resistance to MPTP metabolite MPP+ [53]. VMAT-2 has two binding sites, one with high affinity for reserpine and another one with high affinity to dihydrotetrabenazine and low affinity for reserpine [54]. Aminochrome uptake mediated by VMAT-2 was inhibited by lobeline but not reserpine while dopamine was inhibited by both VMAT-2 inhibitors. Lobeline is an inhibitor of VMAT-2 that specifically interacts on the dihydrotetrabenazine binding site to inhibit dopamine uptake into synaptic vesicles [55]. Our results also show that aminochrome prevents dopamine uptake into monoaminergic vesicles, increasing free cytosolic dopamine and its subsequent oxidation to aminochrome.

5. Conclusions

Our data show that overexpression of VMAT-2 and DT-diaphorase in RCSN3VMAT2GFPDT cells (i) strongly decreases the aminochrome-induced cell death; (ii)

prevents mitochondria inner membrane remodeling; (iii) prevents a decrease in ATP level; (iii) decreases level of autophagy; (iv) decreases DNA laddering; and (v) decreases nDNA damage. Therefore, our results support the idea that VMAT-2 and DT-diaphorase are an important cellular defense against aminochrome-dependent neurotoxicity that could increase vulnerability of neuromelanin containing neurons of the substantia nigra, neurons that selectively degenerate during Parkinson's disease. Neuromelanin formation itself is not a toxic pathway, since this pigment is present in the substantia nigra of individuals not affected with Parkinson's disease, but it is depending on the existence of a defense mechanism such as VMAT-2 and DT-diaphorase that prevent that aminochrome participates in neurotoxic reactions.

Acknowledgments

This work was supported by FONDECYT grants no. 1061083, 1100165 (Chile), and 1F32ES019008-01 to (L.H.S.), and to (J.T.G.). We thank Professor Eduardo Couve of Valparaiso University for valuable discussion related to our studies with transmission electron microscopy. The authors would also like to thank Dr. Pablo Caviedes, who provided the cell line RCSN-3. For any request of this cell line, please contact him directly by e-mail: pablo.caviedes@cicef.cl.

References

1. Chaudhry F, Edwards R, Fonnum F. Vesicular neurotransmitter transporters as targets for endogenous and exogenous toxic substance. Annu Rev Pharmacol Toxicol. 2008; 48:277–301. [PubMed: 17883368]
2. Knoth J, Zallakian M, Njus D. Stoichiometry of H+-linked dopamine transport in chromaffin granule ghost. Biochemistry. 1981; 206:625–6629.
3. Guillot TS, Miller GW. Protective actions of the vesicular monoamine transporter 2 (VMAT2) in monoaminergic neurons. Mol Neurobiol. 2009; 39:149–170. [PubMed: 19259829]
4. Linert W, Herlinger E, Jameson RF, Kienzl E, Jellinger K, Youdim MB. Dopamine 6-hydroxydopamine iron and dioxygen—their mutual interactions and possible implication in the development of Parkinson's disease. Biochim Biophys Acta. 1996; 1316:160–168. [PubMed: 8781534]
5. Krasnova IN, Cadet JL. Methamphetamine toxicity and messengers of death. Brain Res Rev. 2009; 60:379–407. [PubMed: 19328213]
6. Zecca L, Fariello R, Riederer P, Sulzer D, Gatti A, Tampellini D. The absolute concentration of nigral neuromelanin assayed by a new sensitive method increases throughout the life and is dramatically decreased in Parkinson's disease. FEBS Lett. 2002; 510:216–220. [PubMed: 11801257]
7. Zecca L, Stroppolo A, Gatti A, Tampellini D, Toscani M, Gallorini M, Giaveri G, Arosio P, Santambrogio P, Fariello RG, Karatekin E, Kleinman MH, Turro N, Hornykiewicz O, Zucca FA. The role of iron and copper molecules in the neuronal vulnerability of locus coeruleus and substantia nigra during aging. Proc Natl Acad Sci U S A. 2004; 101:9843–9848. [PubMed: 15210960]
8. Kastner A, Hirsch EC, Lejeune O, Javoy-Agid F, Rascol O, Agid Y. Is the vulnerability of neurons in the substantia nigra of patients with Parkinson's disease related to their neuromelanin content? J Neurochem. 1992; 59:1080–1089. [PubMed: 1494900]
9. Gibb WR. Melanin tyrosine hydroxylase calbindin and substance P in the human midbrain and substantia nigra in relation to nigrostriatal projections and differential neuronal susceptibility in Parkinson's disease. Brain Res. 1992; 581:283–291. [PubMed: 1382801]
10. Conway K, Rochet JC, Bieganski RM, Lansbury PT. Kinetic stabilization of the α-synuclein adducts. Science. 2001; 294:1346–1349. [PubMed: 11701929]
11. Norris EH, Giasson BI, Hodara R, Xu S, Trojanowski JQ, Ischiropoulos H, Lee VM. Reversible inhibition of alpha-synuclein fibrillization by dopaminochrome-mediated conformational alterations. J Biol Chem. 2005; 280:21212–21219. [PubMed: 15817478]

12. Van Laar VS, Mishizen AJ, Cascio M, Hastings TG. Proteomic identification of dopamine-conjugated proteins from isolated rat brain mitochondria and SH-SY5Y cells. Neurobiol Dis. 2009; 34:487–500. [PubMed: 19332121]
13. Zafar KS, Siegel D, Ross D. A potential role for cyclized quinones derived from dopamine DOPA and 34-dihydroxyphenylacetic acid in proteasomal inhibition. Mol Pharmacol. 2006; 70:1079–1086. [PubMed: 16790533]
14. Zhou ZD, Lim TM. Dopamine (DA) induced irreversible proteasome inhibition via DA derived quinines. Free Radic Res. 2009; 43:417–430. [PubMed: 19291591]
15. Paris I, Perez-Pastene C, Cardenas S, Iturriaga-Vasquez P, Muñoz P, Couve E, Caviedes P, Segura-Aguilar J. Aminochrome induces disruption of actin alpha- and beta-tubulin cytoskeleton networks in substantia-nigra-derived cell line. J Neurotox Res. 2010; 18:82–92.
16. Arriagada C, Paris I, Sanchez de las Matas MJ, Martinez-Alvarado P, Cardenas S, Castaneda P, Graumann R, Perez-Pastene C, Olea-Azar C, Couve E, Herrero MT, Caviedes P, Segura-Aguilar J. On the neurotoxicity mechanism of leukoaminochrome *o*-semiquinone radical derived from dopamine oxidation: mitochondria damage, necrosis and hydroxyl radical formation. Neurobiol Dis. 2004; 16:468–477. [PubMed: 15193303]
17. Fon EA, Pothos EN, Sun BC, Killeen N, Sulzer D, Edwards RH. Vesicular transport regulates monoamine storage and release but is not essential for amphetamine action. Neuron. 1997; 19:1271–1283. [PubMed: 9427250]
18. Taylor TN, Caudle WM, Miller GW. VMAT2-deficient mice display nigral and extranigral pathology and motor and nonmotor symptoms of Parkinson's disease. Parkinsons Dis. 2011; 2011:124–165.
19. Sulzer D, Bogulavsky J, Larsen KE, Behr G, Karatekin E, Kleinman MH, Turro N, Krantz D, Edwards RH, Greene LA, Zecca L. Neuromelanin biosynthesis is driven by excess cytosolic catecholamines not accumulated by synaptic vesicles. Proc Natl Acad Sci U S A. 2000; 97:11869–11874. [PubMed: 11050221]
20. Liang CL, Nelson O, Yazdani U, Pasbakhsh P, German DC. Inverse relationship between the contents of neuromelanin pigment and the vesicular monoamine transporter-2: human midbrain dopamine neuron. J Comp Neurol. 2004; 473:97–106. [PubMed: 15067721]
21. Segura-Aguilar J, Lind C. On the mechanism of Mn^{3+} induce neurotoxicity of dopamine: prevention of quinone derived oxygen toxicity by DT-diaphorase and superoxide dismutase. Chem Biol Interact. 1989; 72:309–324. [PubMed: 2557982]
22. Lozano J, Muñoz P, Nore BF, Ledoux S, Segura-Aguilar J. Stable expression of short interfering RNA for DT-diaphorase induces neurotoxicity. Chem Res Toxicol. 2010; 23:1492–1496. [PubMed: 20849151]
23. Paris I, Muñoz P, Huenchuguala S, Couve E, Sanders LH, Greenamyre JT, Caviedes P, Segura-Aguilar J. Autophagy protects against aminochrome-induced cell death in substantia nigra-derived cell line. Toxicol Sci. 2011; 121:376–388. [PubMed: 21427056]
24. Fuentes P, Paris I, Nassif M, Caviedes P, Segura-Aguilar J. Inhibition of VMAT-2 and DT-diaphorase induce cell death in a substantia Nigra-derived cell line—an experimental cell model for dopamine toxicity studies. Chem Res Toxicol. 2007; 20:776–783. [PubMed: 17425337]
25. Cardenas SP, Perez-Pastene C, Couve E, Segura-Aguilar J. The DT-diaphorase prevents the aggregation of a-synuclein induced by aminochrome. Neurotox Res. 2008; 13:136.
26. Segura-Aguilar J, Cardenas S, Riveros A, Fuentes-Bravo P, Lozano J, Graumann R, Paris I, Nassif M, Caviedes I. DT-Diaphorase prevents the formation of alpha-synuclein adducts with aminochrome. Soc Neurosci Abstr. 2006; 824:17.
27. Paris I, Dagnino-Subiabre A, Marcelain K, Bennett LB, Caviedes P, Caviedes R, Olea-Azar C, Segura-Aguilar J. Copper neurotoxicity is dependent on dopamine-mediated copper uptake and one-electron reduction of aminochrome in a rat substantia nigra neuronal cell line. J Neurochem. 2001; 77:519–529. [PubMed: 11299314]
28. Dagnino-Subiabre A, Marcelain K, Arriagada C, Paris I, Caviedes P, Caviedes R, Segura-Aguilar J. Mol Cell Biochem. 2000; 212:131–134. [PubMed: 11108144]
29. Segura-Aguilar J, Kaiser R, Lind C. Separation and characterization of isoforms of DT-diaphorase from rat liver cytosol. Biochim Biophys Acta. 1992; 1120:33–42. [PubMed: 1372830]

30. Ayala-Torres S, Chen Y, Svoboda T, Rosenblatt J, Van Houten B. Analysis of gene-specific DNA damage and repair using quantitative polymerase chain reaction. Methods. 2000; 22:135–147. [PubMed: 11020328]
31. Santos JH, Meyer JN, Mandavilli BS, Van Houten B. Quantitative PCR-based measurement of nuclear and mitochondrial DNA damage and repair in mammalian cells. Methods Mol Biol. 2006; 314:183–199. [PubMed: 16673882]
32. Williams A. MPTP parkinsonism. Br Med J. 1984; 289:1401–1402. [PubMed: 6437573]
33. Zhang W, Phillips K, Wielgus AR, Liu J, Albertini A, Zucca FA, Faust R, Qian SY, Miller DS, Chignell CF, Wilson B, Jackson-Lewis V, Przedborski S, Joset D, Loike J, Hong JS, Sulzer D, Zecca L. Neuromelanin activates microglia and induces degeneration of dopaminergic neurons: implications for progression of Parkinson's disease. Neurotox Res. 2011; 19:63–72. [PubMed: 19957214]
34. Zecca L, Wilms H, Geick S, Claasen JH, Brandenburg LO, Holzknecht C, Panizza ML, Zucca FA, Deuschl G, Sievers J, Lucius R. Human neuromelanin induces neuroinflammation and neurodegeneration in the rat substantia nigra: implications for Parkinson's disease. Acta Neuropathol. 2008; 116:47–55. [PubMed: 18343932]
35. LaVoie MJ, Ostaszewski BL, Weihofen Schlossmacher A, Selkoc DJ. Dopamine covalently modifies and functionally inactivates parkin. Nat Med. 2005; 11:1159–1161. [PubMed: 16270070]
36. Xu Y, Stokes AH, Roskoski R, Vrana K. Dopamine in the presence of tyrosinase covalently modifies and inactivates tyrosinase hydroxylase. J Neurosci Res. 1998; 54:691–697. [PubMed: 9843160]
37. Whitehead R, Ferrer JV, Javitch JA, Justice JB. Reaction of oxidized dopamine whit endogenous cysteine residues in the human dopamine transporter. J Neurochem. 2001; 76:1242–1251. [PubMed: 11181843]
38. Paris I, Cárdenas S, Lozano J, Perez-Pastene C, Graumann R, Caviedes P, Segura-Aguilar J. Aminochrome as a preclinical experimental model to study degeneration of dopaminergic neurons in Parkinson's disease. Neurotox Res. 2007; 13:221–230. [PubMed: 18522901]
39. Cartier EA, Parra LA, Baust TB, Quiroz M, Salazar G, Faundez V, Egaña L, Torres GE. A biochemical and functional protein complex involving dopamine synthesis and transport into synaptic vesicles. J Biol Chem. 2010; 15:1957–1966. [PubMed: 19903816]
40. Chen JJ, Wilkinson JR. The monoamine oxidase type B inhibitor rasagiline in the treatment of Parkinson disease: is tyramine a challenge? J Clin Pharmacol. May 31.2011 Electronic publication ahead of print. 10.1177/0091270011406279
41. Baez S, Linderson Y, Segura-Aguilar J. Superoxide dismutase and catalase enhance autoxidation during one-electron reduction of aminochrome by NADPH-cytochrome P-450 reductase. Biochem Mol Med. 1995; 54:12–18. [PubMed: 7551811]
42. Segura-Aguilar J, Metodiewa D, Welch CJ. Metabolic activation of dopamine *o*quinones to *o*-semiquinones by NADPH cyytochrome P450 reductase may play an important role in oxidative stress and apoptotic effects. Biochim Biophys Acta. 1998; 1381:1–6. [PubMed: 9659366]
43. Matsui Y, Kyoi S, Takagi H, Hsu CP, Hariharan N, Ago T, Vatner SF, Sadoshima J. Molecular mechanisms and physiological significance of autophagy during myocardial ischemia and reperfusion. Autophagy. 2008; 4:409–415. [PubMed: 18227645]
44. Tettamanti G, Saló E, González-Estévez C, Felix DA, Grimaldi A, de Eguileor M. Autophagy in invertebrates: insights into development, regeneration and body remodeling. Curr Pharm Des. 2008; 14:116–125. [PubMed: 18220823]
45. Kuma A, Mizushima N. Physiological role of autophagy as an intracellular recycling system: with an emphasis on nutrient metabolism. Semin Cell Dev Biol. 2010; 21:683–690. [PubMed: 20223289]
46. Seglen PO, Brinchmann MF. Purification of autophagosomes from rat hepatocytes. Autophagy. 2010; 6:542–547. [PubMed: 20505360]
47. Schmelzle T, Hall MN. TOR, a central controller of cell growth. Cell. 2000; 103:253–262. [PubMed: 11057898]

48. Caudle WM, Richardson JR, Wang MZ, Taylor TN, Guillot TS, McCormack AL, Colebrooke RE, Di Monte DA, Emson PC, Miller GW. Reduced vesicular storage of dopamine causes progressive nigrostriatal neurodegeneration. J Neurosci. 2007; 27:8138–8148. [PubMed: 17652604]

49. Vergo S, Johansen JL, Leist M, Lotharius J. Vesicular monoamine transporter 2 regulates the sensitivity of rat dopaminergic neurons to disturbed cytosolic dopamine levels. Brain Res. 2007; 1185:18–32. [PubMed: 18028884]

50. Guillot TS, Shepherd KR, Richardson JR, Wang MZ, Li Y, Emson PC, Miller GW. Reduced vesicular storage of dopamine exacerbates methamphetamine-induced neurodegeneration and astrogliosis. J Neurochem. 2008; 106:2205–2217. [PubMed: 18643795]

51. Nakagawa T, Suzuki Y, Nagayasu K, Kitaichi M, Shirakawa H, Kaneko S. Repeated exposure to methamphetamine, cocaine or morphine induces augmentation of dopamine release in rat mesocorticolimbic slice co-cultures. PLoS One. 2011; 6:24865.

52. Gainetdinov RR, Fumagalli F, Wang YM, Jones SR, Levey AI, Miller GW, Caron MG. Increased MPTP neurotoxicity in vesicular monoamine transporter 2 heterozygote knockout mice. J Neurochem. 1998; 70:1973–1978. [PubMed: 9572281]

53. Adam Y, Edwards RH, Schuldiner S. Expression and function of the rat vesicular monoamine transporter 2. Am J Physiol Cell Physiol. 2008; 294:C1004–C1011. [PubMed: 18287335]

54. Scherman D, Henry JP. Reserpine binding to bovine chromaffin granule membranes. Characterization and comparison with dihydrotetrabenazine binding. Mol Pharmacol. 1984; 25:113–122. [PubMed: 6708929]

55. Teng L, Crooks PA, Dwoskin LP. Lobeline displaces [^{3}H]dihydrotetrabenazine binding and releases [^{3}H]dopamine from rat striatal synaptic vesicles: comparison with d-amphetamine. J Neurochem. 1998; 71:258–265. [PubMed: 9648873]

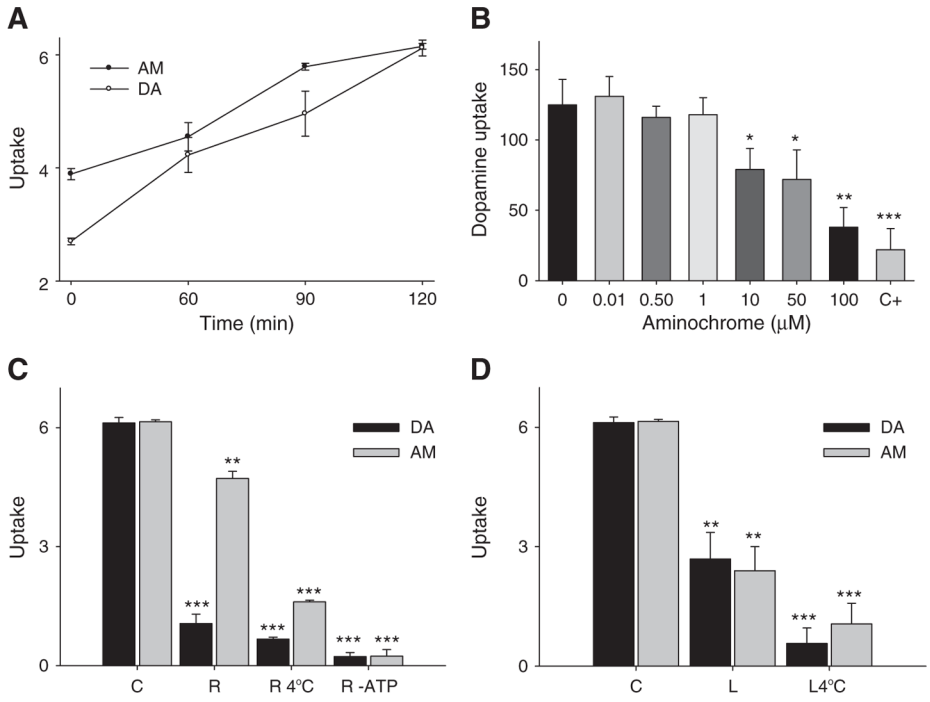

Fig. 1.

Dopamine and aminochrome uptake into synaptic vesicles. (A) The uptake of dopamine and aminochrome into synaptic vesicles was measured in rat brain synaptic vesicles by incubating the vesicles with 50 nM ^{3}H-dopamine or ^{3}H-aminochrome. Brain synaptic vesicles are able to take up both dopamine and aminochrome at similar rate during 0, 60, 90 and 120 min as described under Materials and methods; (B) dopamine uptake inhibition into rat substantia nigra synaptic vesicles in the presence of aminochrome. ^{3}H-Dopamine uptake was measured at different aminochrome concentrations (0, 0.01, 0.5, 1, 10, 50, 100 μM). ^{3}H-Dopamine uptake was inhibited by aminochrome at concentration higher than 10 μM aminochrome. As positive control of dopamine uptake inhibition was used 50 μM (C+); (C) the effect of reserpine on ^{3}H-Dopamine or ^{3}H-aminochrome uptake in rat brain synaptic vesicles was determined at 120 min in the presence of cell culture medium (C); 1 μM reserpine at 37 °C (R) at 4 °C (R 4 °C) or in the absence of ATP (R-ATP); (D) the effect of lobeline on uptake of ^{3}H-dopamine or ^{3}H-aminochrome into rat substantia nigra synaptic vesicles was determined at 120 min at 37 °C in the presence of cell culture medium (C); in the presence of 2 μM lobeline at 37 °C (L) or at 4 °C (L 4 °C). The values are the mean ± SD and the statistical significance was assessed using ANOVA for multiple comparisons and Student's *t* test (***P<0.001; **P<0.01; *P<0.05).

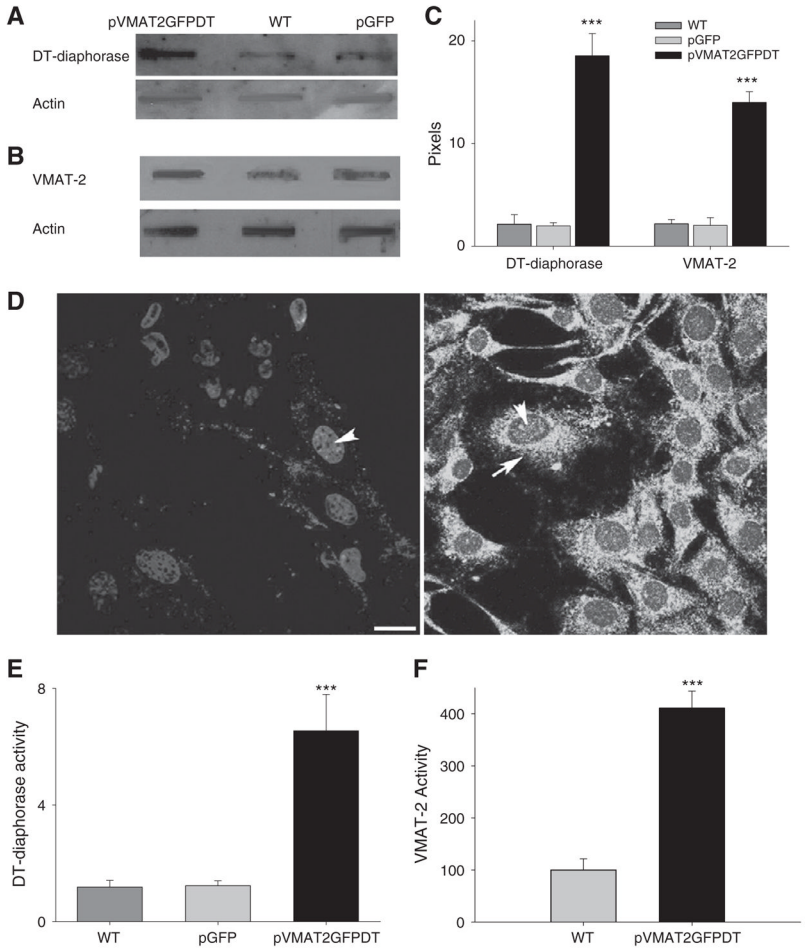

Fig. 2.

Over-expression of VMAT-2 and DT-diaphorase in RCSN-3 cells. (A) The expression of DT-diaphorase (A) and VMAT2 (B) in RCSN-3 cells transfected with pVMAT2GFPDT was determined by using dot blot technique. As control RCSN-3 cells (WT) and RCSN-3 transfected with pGFP were used (pGFP). Antibodies against DT-diaphorase, VMAT-2 and actin were used to determine their expression as described under Materials and methods. (C) Quantification of expression of VMAT-2 and DT-diaphorase were determined by using the software Scion Image (NIH) and the values correspond to pixels of DT-diaphorase or VMAT-2/pixels of actin. (D) The green fluorescence of GFP (arrow) in all RCSN3VAMT2GFPDT cells (right) contrasts with the lack of fluorescence in RCSN-3 cells (left). The nucleus was stained in both RCSN-3 and RCSN3VAMT2GFPDT cells with DAPI staining (head of arrows; bar = 10 μm); (E) DT-diaphorase activity was determined by using NADH and menadione as electron donator and acceptor as described under Materials and methods. (F) VMAT-2 activity was determined by using ^{3}H-dopamine as described in Materials and methods. The statistical significance was assessed using ANOVA for multiple comparisons and Student's *t* test (***P<0.001).

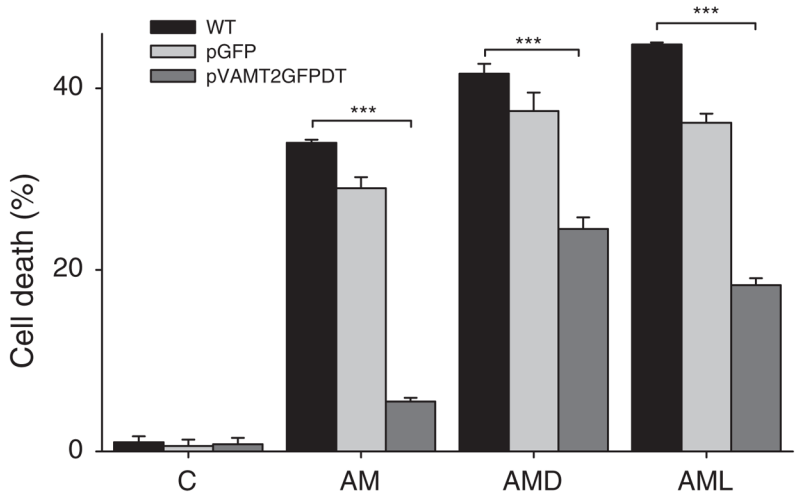

Fig. 3.

Aminochrome induced cell death in RCSN-3 RCSN-3-GFP and RCSN-3VMAT2GFPDT and cell lines in the presence of aminochrome, dicoumarol and lobeline. The cell death was determined in RCSN-3, RCSN-3-GFP or RCSN3VMAT2GFPDT cells incubated during 24 h with cell culture medium (C) 20 μM aminochrome (AM) 20 μM aminochrome and 100 μM dicoumarol (AMD) 20 μM aminochrome and 2 μM lobeline (AML) as described under Materials and methods. Our results show that RCSN3VMAT2GFPDT cells overexpressing VMAT-2 and DT-diaphorase are resistant to aminochrome neurotoxicity. The statistical significance was assessed using ANOVA for multiple comparisons and Student's *t* test (***P<0.001).

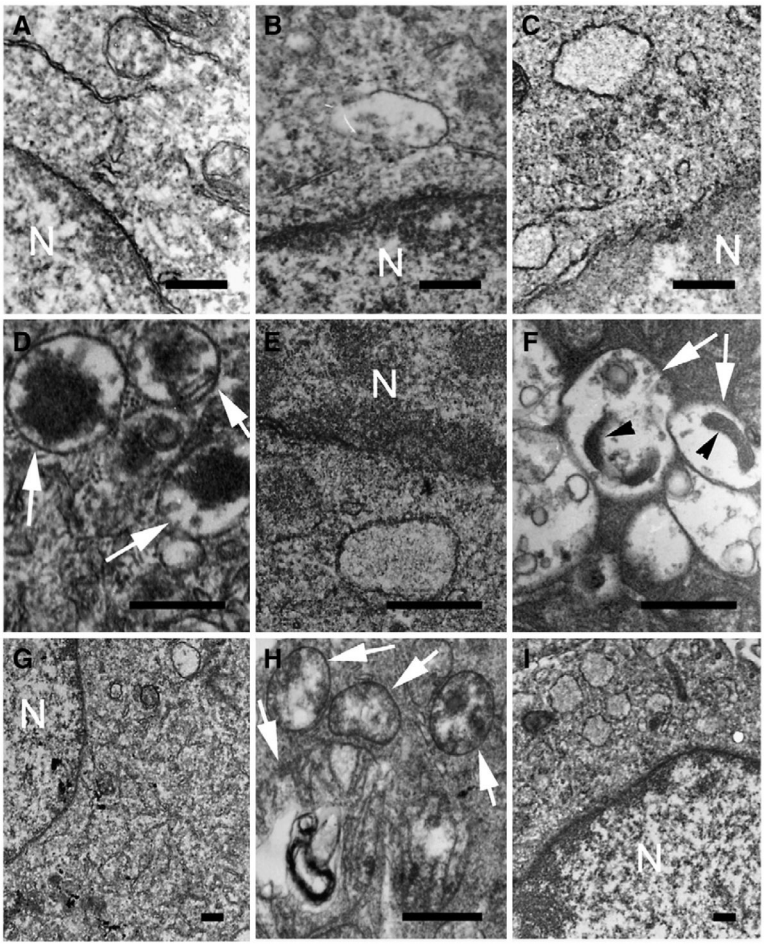

Fig. 4.

Ultrastructural analysis of autophagic vacuoles in RCSN-3 and RCSN3VMAT2GFPDT cells treated with aminochrome, dicoumarol and lobeline. The formation of autophagic vacuoles (white arrows) in RCSN-3 and RCSN3VMAT2GFPDT cells was determined by using transmission electron microscopy in RCSN-3 cells incubated during 24 h with cell culture medium (A) 100 μM dicoumarol (B) 2 μM lobeline (C) 20 μM aminochrome (D) 20 μM aminochrome and 100 μM dicoumarol (F) and 20 μM aminochrome and 2 μM lobeline (H). RCSN3VMAT2GFPDT cells incubated with 20 μM aminochrome (E) 20 μM aminochrome and 100 μM dicoumarol (G) and 20 μM aminochrome and 2 μM lobeline (I). (Bars = 0.5 μm; nucleus N).

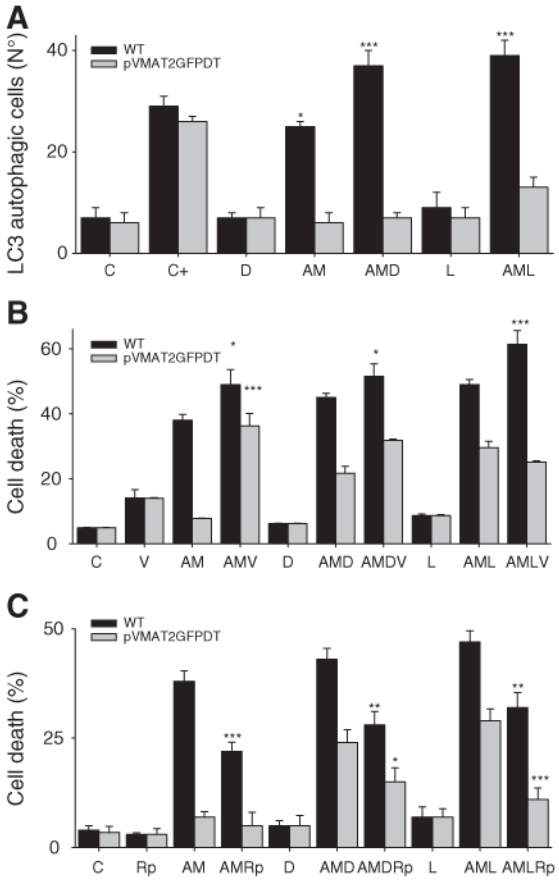

Fig. 5.

Autophagy role in aminochrome-induced cell death in RCSN-3 and RCSN3VMAT2GFPDT cells. (A) The effect of aminochrome on autophagy was determined by transfecting RCSN-3 and RCSN3VMAT2GFPDT cells with a plasmid coding for LC3-GFP. A statistical significant decrease in autophagy was observed in RCSN3VMAT2GFPDT cells with high expression of both VMAT-2 and DT-diaphorase in comparison with RCSN-3 cells when the cells were incubated with 20 μM aminochrome (AM); 20 μM aminochrome and 2 μM lobeline (AML); 20 μM aminochrome and 100 μM dicoumarol (AMD); and 20 μM aminochrome 100 μM dicoumarol and 2 μM lobeline (AMDL). No significant difference was observed between these cell lines when these cells were incubated with cell culture medium in the presence (C) and the absence of bovine serum (C+) 100 μm dicoumarol (D) 2 μM lobeline (L); (B) the effect of vinblastine on aminochrome induced death was determined in RCSN-3 and RCSN3VMAT2GFPDT. The cells were incubated 20 μM aminochrome (AM) 20 μM aminochrome and 10 μM vinblastine (AMV) 20 μM aminochrome and 100 μM dicoumarol (AMD) 20 μM aminochrome 100 μM dicoumarol and 10 μM vinblastine (AMDV) 20 μM aminochrome and 2 μM lobeline (AML) 20 μM aminochrome 2 μM lobeline and 10 μM vinblastine 10 μM vinblastine (V) 100 μM dicoumarol (D) and 2 μM lobeline (L). The presence of vinblastine increased aminochrome-induced cell death both in RCSN-3 and RCSN3VMAT2GFPDT; (C) the effect of rapamycin on aminochrome induced death was determined in RCSN-3 and RCSN3VMAT2GFPDT. The cells were incubated 20 μM aminochrome (AM), 20 μM aminochrome and 10 μM rapamycin (AMR); 20 μM aminochrome and 100 μM dicoumarol (AMD); 20 μM aminochrome 100 μM dicoumarol and 10 μM rapamycin (AMDR); 20 μM aminochrome and 2 μM lobeline (AML); 20 μM aminochrome 2 μM lobeline and 10 μM rapamycin; 10

μM rapamycin (R); 100 μM dicoumarol (D); 2 μM lobeline (L). The presence of rapamycin decreased aminochrome-induced cell death both in RCSN-3 and RCSN3VMAT2GFPDT. The statistical significance was assessed using ANOVA for multiple comparisons and Student's *t* test (*P<0.05; **P<0.01; ***P<0.001).

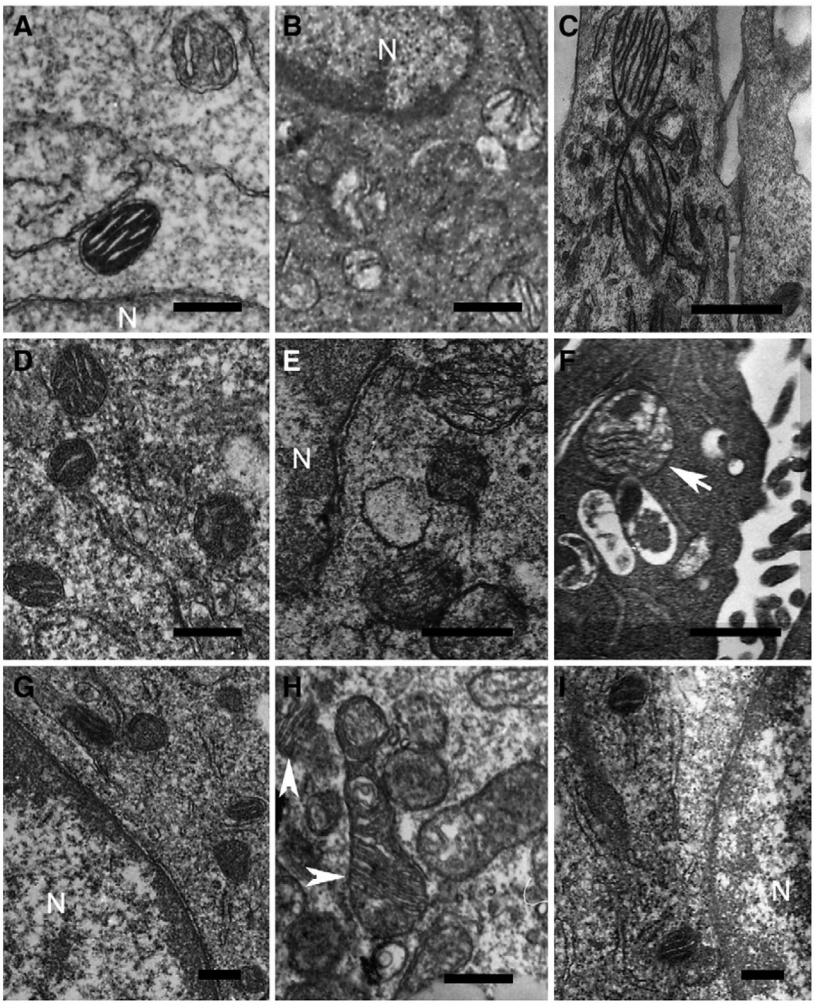

Fig. 6.

Mitochondria ultrastructural analysis in RCSN-3 and RCSN-3VMAT2GFPDT cells treated with aminochrome. Normal mitochondria inner membranes were observed in RCSN-3 cells incubated during 24 h with cell culture medium (A); 100 μM dicoumarol (B); 2 μM lobeline (C) and 20 μM aminochrome (D) or in RCSN3VMAT2GFPDT cells treated with 20 μM aminochrome (E). However, remodeling of the inner membrane conformation in mitochondrial ultrastructure were observed in RCSN-3 cells treated with 20 μM aminochrome and 100 μM dicoumarol; (F) or 20 μM aminochrome and 2 μM lobeline; (H) contrasting with normal mitochondria ultra structure in RCSN3VMAT2GFPDT cells treated under the same conditions (G and I) respectively. (Bars = 0.5 μm; nucleus N).

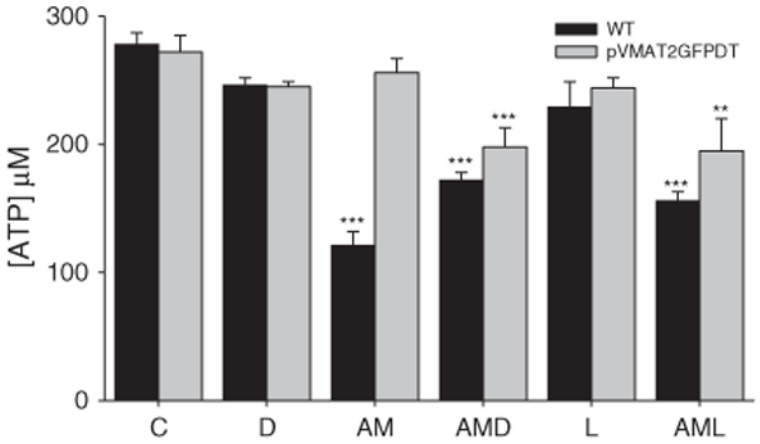

Fig. 7.

The effect of aminochrome on intracellular ATP level in RCSN-3 and RCSN-3VMAT2GFPDT cells. A significant decrease in ATP level was observed in RCSN-3 cells treated with 20 μM aminochrome (AM) contrasting with the lack of effect in RCSN3VMAT2GFPDT cells treated under the same conditions. The cells were treated with cell culture medium (C); 100 μm dicoumarol (D); 20 μM aminochrome and 100 μM dicoumarol (AMD); 2 μM lobeline (L); and 20 μM aminochrome and 2 μM lobeline (AML). The statistical significance was assessed using ANOVA for multiple comparisons and Student's *t* test (**P<0.01; ***P<0.001).

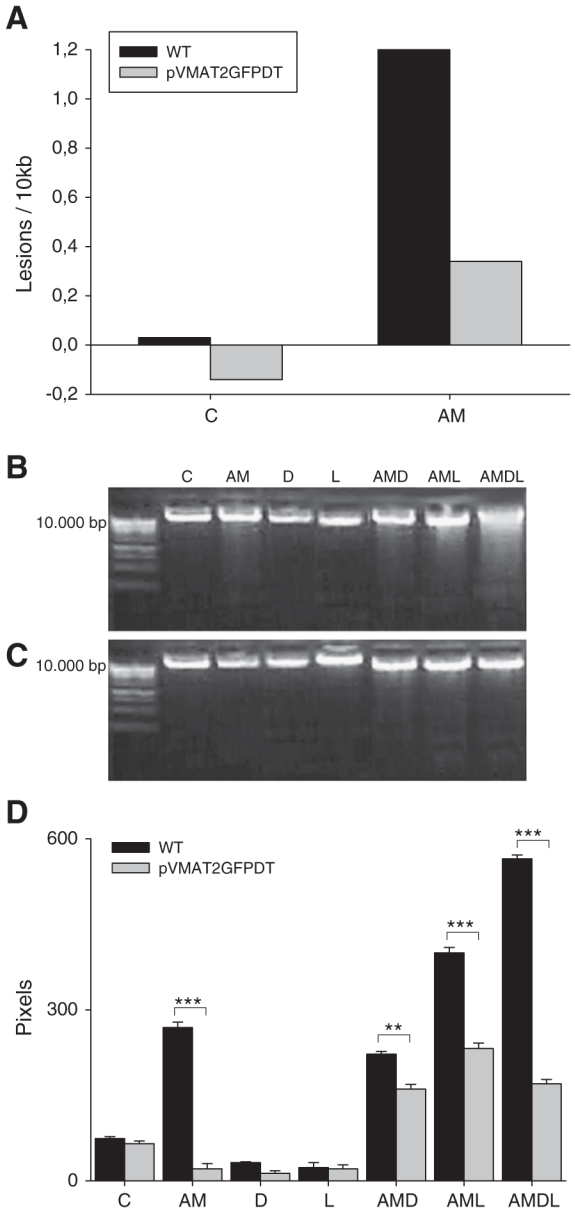

Fig. 8.

The effect of aminochrome on DNA. (A) Nuclear DNA damage was decreased in RCSN3VMAT2GFPDT cells treated with 20 μM aminochrome (AM) or cell culture medium (C) in comparison to RCSN-3 cells treated under the same conditions; (B) a significant decrease in DNA fragmentation was observed in cells RCSN3VMAT2GFPDT in comparison with RCSN-3 cells treated with 20 μM aminochrome (AM); 20 μM aminochrome and 100 μM dicoumarol (AMD); 20 μM aminochrome and 2 μM lobeline (AML); 20 μM aminochrome, 100 μM dicoumarol and 2 μM lobeline (AMDL). As control the cells were treated with 2 μM lobeline (L) or 100 μM dicoumarol (D). The statistical significance was assessed using ANOVA for multiple comparisons and Student's *t* test (***P<0.001).

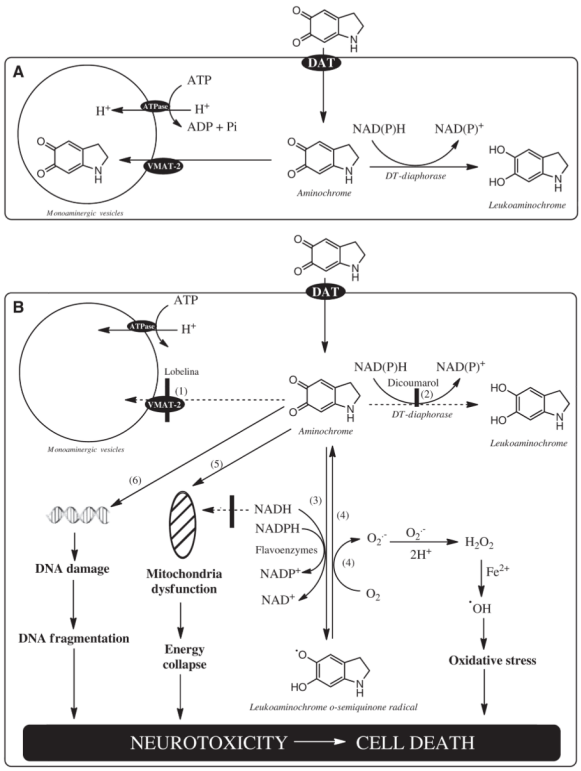

Fig. 9.

Possible role of VMAT-2 and DT-diaphorase in aminochrome neurotoxicity. (A) RCSN3VMAT2GFPDT cells with overexpression of VMAT-2 and DT-diaphorase prevent aminochrome neurotoxicity by transporting aminochrome into monoaminergic vesicles catalyzed by VMAT-2 a reaction that requires ATP and/or by reducing aminochrome with two-electron catalyzed by DT-diaphorase. These two enzymes provides protection against aminochrome neurotoxicity; (B) RCSN-3 cells with constitutive level of expression of VMAT-2 and DT-diaphorase or when VMAT-2 and DT-diaphorase are inhibited by lobeline (reaction 1) and dicoumarol (reaction 2) respectively aminochrome is able to (i) form adducts with proteins such as complex I and complex III of electron transport chain in mitochondria inhibiting ATP production in mitochondria (reaction 5); (ii) damage DNA and subsequent fragmentation (reaction 6); (iii) be one-electron reduced catalyzed by flavoenzymes that use NADH as a electron donator generating leukoaminochrome *o*-semiquinone radical (reaction 3) that is extremely reactive with oxygen creating a redox cycling between aminochrome and leukoaminochrome *o*-semiquinone radical (reaction 4) that continues until NADH and oxygen are depleted affecting the ATP production in the electron transport chain. Aminochrome can also be one-electron reduced by flavoenzymes that use NADP as electron donator resulting in the depletion of NADPH required for several biosynthetic reaction and reduction of oxidized glutathione. All these reactions finally induce cell death.